Isotopic control over self-assembly in supramolecular gels

McAulay, Kate; Wang, Han; Fuentes-Caparrós, Ana M.; Thomson, Lisa; Khunti, Nikul; Cowieson, Nathan ; Cui, Honggang; Seddon, Annela; Adams, Dave J

Published in:
Langmuir

DOI:
10.1021/acs.langmuir.0c01552

Publication date:
2020

Document Version
Publisher's PDF, also known as Version of record

LANGMUIR

pubs.acs.org/Langmuir Article

Isotopic Control over Self-Assembly in Supramolecular Gels

Kate McAulay, Han Wang, Ana M. Fuentes-Caparrós, Lisa Thomson, Nikul Khunti, Nathan Cowieson, Honggang Cui, Annela Seddon, and Dave J. Adams*

Cite This: *Langmuir* 2020, 36, 8626–8631 Read Online

ACCESS | Metrics & More | Article Recommendations | Supporting Information

ABSTRACT: It is common to switch between H_2O and D_2O when examining peptide-based systems, with the assumption being that there are no effects from this change. Here, we describe the effect of changing from H_2O to D_2O in a number of low-molecular-weight dipeptide-based gels. Gels are formed by decreasing the pH. In most cases, there is little difference in the structures formed at high pH, but this is not universally true. On lowering the pH, the kinetics of gelation are affected and, in some cases, the structures underpinning the gel network are different. Where there are differences in the self-assembled structures, the resulting gel properties are different. We, therefore, show that isotopic control over gel properties is possible.

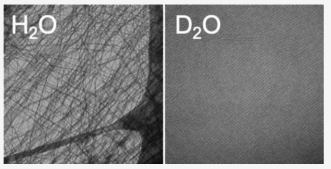

Low-molecular-weight, or supramolecular, gels are formed by the self-assembly of small molecules into fibers that subsequently entangle.[1−4] The assembly is driven by noncovalent interactions including hydrogen bonding, hydrophobicity, and π-stacking. As such, very small changes in molecular structure often lead to dramatic differences. It is therefore unsurprising that each molecule has solvent-dependent gelation efficiency.[1]

For hydrogels, hydrophobicity and hydrogen bonding are dominant noncovalent interactions.[5] On changing from H_2O to D_2O, a number of properties change, including density, viscosity, and hydrogen bond strength.[6] Additionally, the hydrophobic effect has also been reported to be more pronounced in D_2O than in H_2O.[7] In some systems, substituting H_2O for D_2O can lead to a change in properties. For example, the persistence length of elastic peptides is higher in D_2O than that in H_2O, ascribed to stronger hydrogen bonding.[8] Slight differences in dimensions have been reported for nanotubes formed from a small peptide in H_2O or D_2O.[9] For biopolymer-based gels, the melting temperature of gelatin gels is higher in D_2O as compared to H_2O,[10] and the gels are more rigid in D_2O. Similarly, agar-based gels have a higher modulus in D_2O compared to H_2O,[11] as do κ-carrageenan-based gels.[12] Fibrinogen has been shown to have higher degrees of lateral aggregation in the gel state in D_2O as compared to H_2O.[13] The higher melting points of gelatin gels in D_2O can be ascribed to the enhanced stability of the triple helices[10] and similar increases in melting point have been shown for other biopolymer gels in D_2O compared to H_2O.[12,14] Structural changes have also been observed in lipid systems when changing from H_2O to D_2O.[15]

For low-molecular-weight gels, there is very little information as to whether there is an effect of changing from H_2O to D_2O. Canrinus et al. reported differences in gel strength in some cases when changing from H_2O to D_2O on the basis of gel melting temperatures, which could differ by as much as 50 °C.[16] The rheological data were stated to be essentially the same. Variations in hydrophobicity were assigned as the dominant reason for changes in the melting point.

In addition to the suggestions that it might be possible to change the gel properties when using D_2O instead of H_2O, there are also important implications for a number of experimental techniques. It is common, for example, to carry out infrared spectroscopy in D_2O instead of H_2O to minimize the absorbance of water.[17,18] Likewise, NMR experiments are typically carried out in D_2O. Small-angle neutron scattering (SANS) is most often carried out in D_2O to allow contrast with the gelators.[19,20] In all cases, the often implicit assumption is that this change has no effect.

Here, we focus on a small library of dipeptide-based gelators (Scheme 1).[4,21−26] These form gels in water using a pH-switch. Typically, a solution of one of the gelators is prepared by dispersing the molecule at high pH (pH 10−11) at a concentration of 5 mg/mL. Decreasing the pH results in gelation. The kinetics here control the homogeneity of the gel and so we commonly exploit the hydrolysis of glucono-δ-lactone (GdL) to gluconic acid to lead to a slow, controlled decrease in pH.[27,28] This leads to very reproducible gels.[21] The rate of hydrolysis of GdL has been reported to differ in H_2O and D_2O.[28]

There are therefore primarily two states to be considered where there might be differences in H_2O and in D_2O: the high-pH (solution) phase and the low-pH (gel) phase. It can be difficult to probe these states effectively. It is common to use electron microscopy to image the underlying structures.

Received: May 26, 2020
Revised: July 2, 2020
Published: July 2, 2020

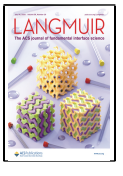

https://dx.doi.org/10.1021/acs.langmuir.0c01552
Langmuir 2020, 36, 8626−8631

Scheme 1. Chemical Structures of the Gelators

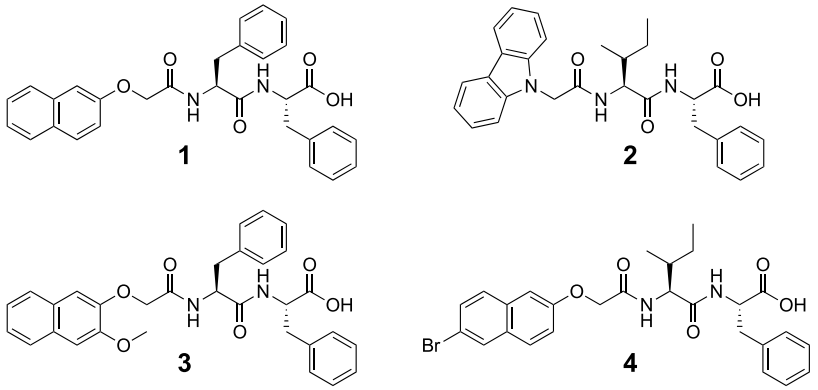

However, there can be drying artifacts for these systems.[29] We, therefore, turned to small-angle X-ray scattering (SAXS).[19] SAXS can be carried out directly on either the solution or gel phase, provides data on the structures of the bulk sample, and can be carried out equally effectively in H_2O and D_2O. We also note here that even small changes in molecular structure can have a profound effect on the outcome of the self-assembly in both the solution and gel states.[2,4,22]

Initially, we focus on the behavior in the solution state at high pH. We have reported previously the assembly of **1** in both H_2O[30] and D_2O,[31] with no major difference observed between the systems. At high pH, at a concentration of 5 mg/mL, **1** forms a viscous solution. In line with previous data, at high pH, the SAXS data (Figure 1a) fit to a flexible cylinder model with radii of 4.1 and 4.3 nm in H_2O and D_2O, respectively, Kuhn lengths of 50 and 77 nm, respectively, and a length outside the scattering length that is accessible from collecting the data over this Q-range. In line with these data, cryo-TEM of the solutions (Figure 1b,c) shows long, flexible structures.

For solutions of **2** at high pH, the best fit to the SAXS data (Figure 1d) is using a hollow cylinder combined with a power law to take into account the scattering at low *Q*. The fits to the data imply that the tubes have radii of 1.7 and 1.9 nm in H_2O and D_2O, respectively, and thicknesses of 3.2 and 2.8 nm, respectively. The cryo-TEM images (Figure 1e,f) agree with the SAXS data, showing long, anisotropic structures. For **3** at high pH, the SAXS (Figure 1g) and cryo-TEM data (Figure 1h,i) again show that very similar structures are formed in H_2O and D_2O. In both cases, the SAXS data can be fitted to a hollow tube model, with radii of 28.1 and 28.7 nm in H_2O and D_2O, respectively, and a thickness of 4.3 nm in each case. Cryo-TEM again backs up the fits to the SAXS data. Finally, for **4** at high pH, there is a difference in the SAXS data (Figure 1j). The model that best fits the SAXS data for the sample in H_2O is a flexible elliptical cylinder with a radius of 1.05 nm and an axis ratio of 3.9, whilst the sample in D_2O is best fit using a flexible cylinder with a radius of 2.6 nm. The cryo-TEM data (Figure 1k,l) backs up the fits to the SAXS data, showing that the structures formed in H_2O and D_2O at high pH are indeed different, with more tapelike structures found in H_2O.

Hence, there is generally little difference in H_2O and D_2O at high pH. There is a general tendency for the radii to be very slightly higher in D_2O, which may be due to solvation differences. Nonetheless, the structures formed are very similar in both solvents. However, for **4**, the structures formed are different.

We now discuss the gels. Gelation was then induced in all cases by the addition of GdL,[27,28] leading to protonation of the terminal carboxylates. The rate of pH decrease is different in H_2O and D_2O, being slower in D_2O (Figure S3, Supporting Information) in all cases. As a result, the times at which gelation begins (where the storage (G') begins to deviate strongly from the loss (G'') modulus) as well as the profiles of G' and G'' are different. In all cases, gelation begins and achieves plateau values at earlier times in H_2O as compared to D_2O, correlating with the slower hydrolysis of GdL in D_2O. The rate of hydrolysis of GdL is catalyzed by many acids and bases, with the relative rate depending on the catalytic species.[28] Since we have a complex solution where aggregates exist and are changing, as well as an evolving pH, the exact species catalyzing the hydrolysis is difficult to determine. Nonetheless, we observe that the hydrolysis in these systems is faster in H_2O than in D_2O (Figure S3) and this directly links to faster gelation in the H_2O compared to that in D_2O. The final gels are visually similar in both H_2O and D_2O (Figure 2). For **1**, although the underlying structures are very similar at high pH (see the discussion above), the viscosities are different, which may be a result of the higher Kuhn length in D_2O as compared to H_2O. This manifests in the sample in D_2O at early times having a storage modulus (G') that is higher than the loss modulus (G'') (Figure 2a). The SAXS data can be used to determine the structures present but will not be easily able to pull out information about interactions between these structures. In H_2O, whilst still viscous, G'' dominates at early times. Since the hydrolysis of GdL is faster in H_2O, changes in G' and G'' occur earlier in the sample in H_2O compared to that in D_2O (Figure 2a). However, the final rheological values of G' and G'' are similar in H_2O and D_2O for the gels formed from **1** (Figure S4). This is expected; we have previously found little differences for gels formed from **1** in both H_2O and D_2O.

However, the final values of G' and G'' differ for gels formed from **2**, **3**, and **4** in H_2O and D_2O. For **2**, the initial solutions are very similar in terms of the values of G' and G'' (Figure 2b) and, whilst the rates of change in the moduli differ in H_2O and D_2O, the moduli for the final gels are relatively similar (Figure S4). For **3**, the initial values of G' and G'' are different, with G' being higher for the solutions in H_2O. The differences in rheological data at early times for **3** show that the interactions between the structures must be stronger in H_2O as compared to those in D_2O since the SAXS data implies that the structures present at high pH are very similar. The final gels are stiffer in H_2O as compared to those in D_2O. For **4**, the initial solutions have higher values of G' and G'' in H_2O compared to those in

https://dx.doi.org/10.1021/acs.langmuir.0c01552
Langmuir 2020, 36, 8626−8631

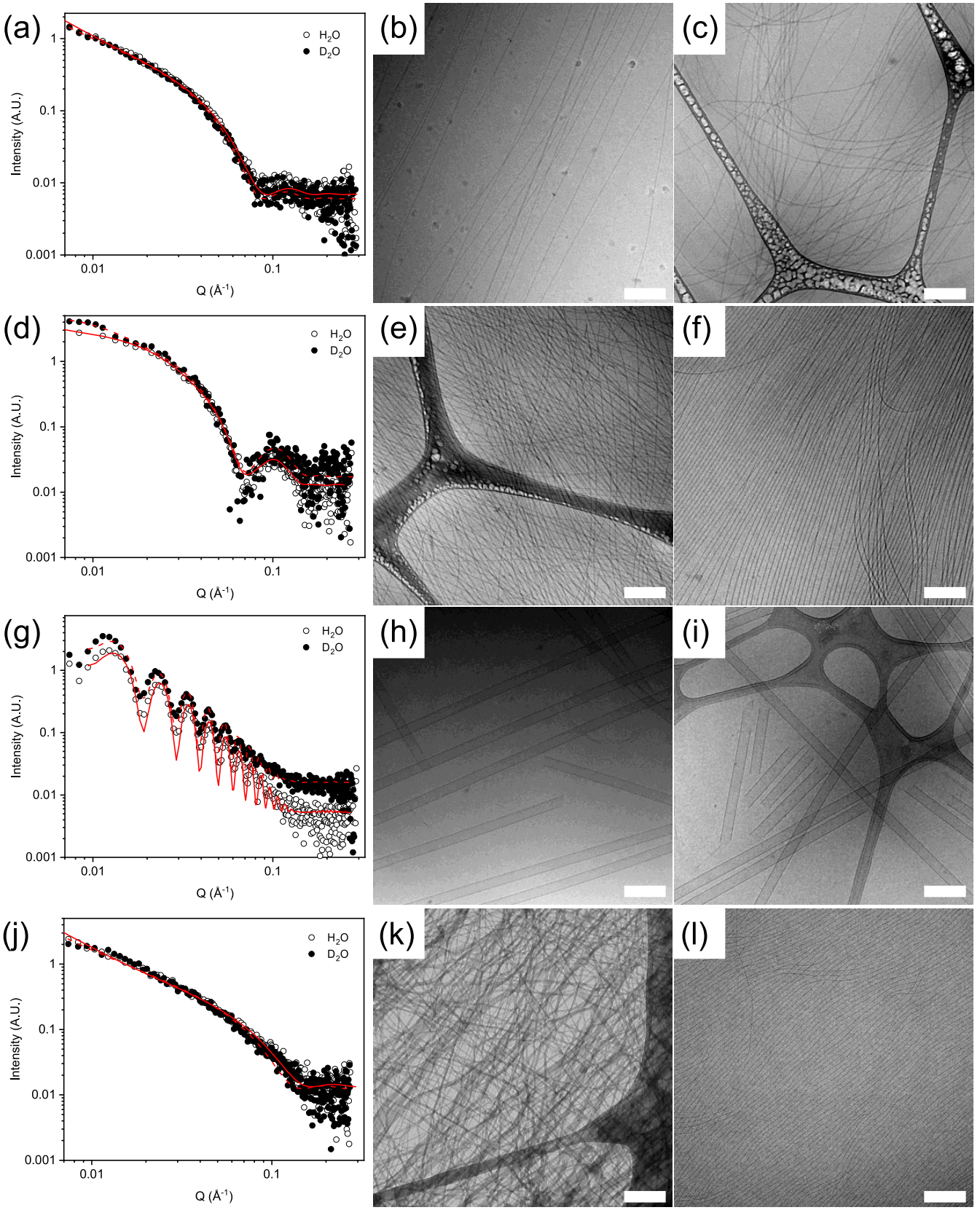

Figure 1. SAXS data and fit for solutions of **1**−**4** in H_2O (open symbols) and D_2O (closed symbols), with fits as red lines: (a) **1**, (d) **2**, (g) **3**, and (j) **4**. Also shown are example cryo-TEM data for solutions of **1**−**4** in H_2O and D_2O: (b) and (c) **1** in H_2O and D_2O, respectively, (e) and (f) **2** in H_2O and D_2O, respectively, (h) and (i) **3** in H_2O and D_2O, respectively, and (k) and (l) **4** in H_2O and D_2O, respectively. All data was collected at a concentration of 5 mg/mL and a pH of 11. For the cryo-TEM data, the scale bars represent 200 nm in each case.

https://dx.doi.org/10.1021/acs.langmuir.0c01552
Langmuir 2020, 36, 8626−8631

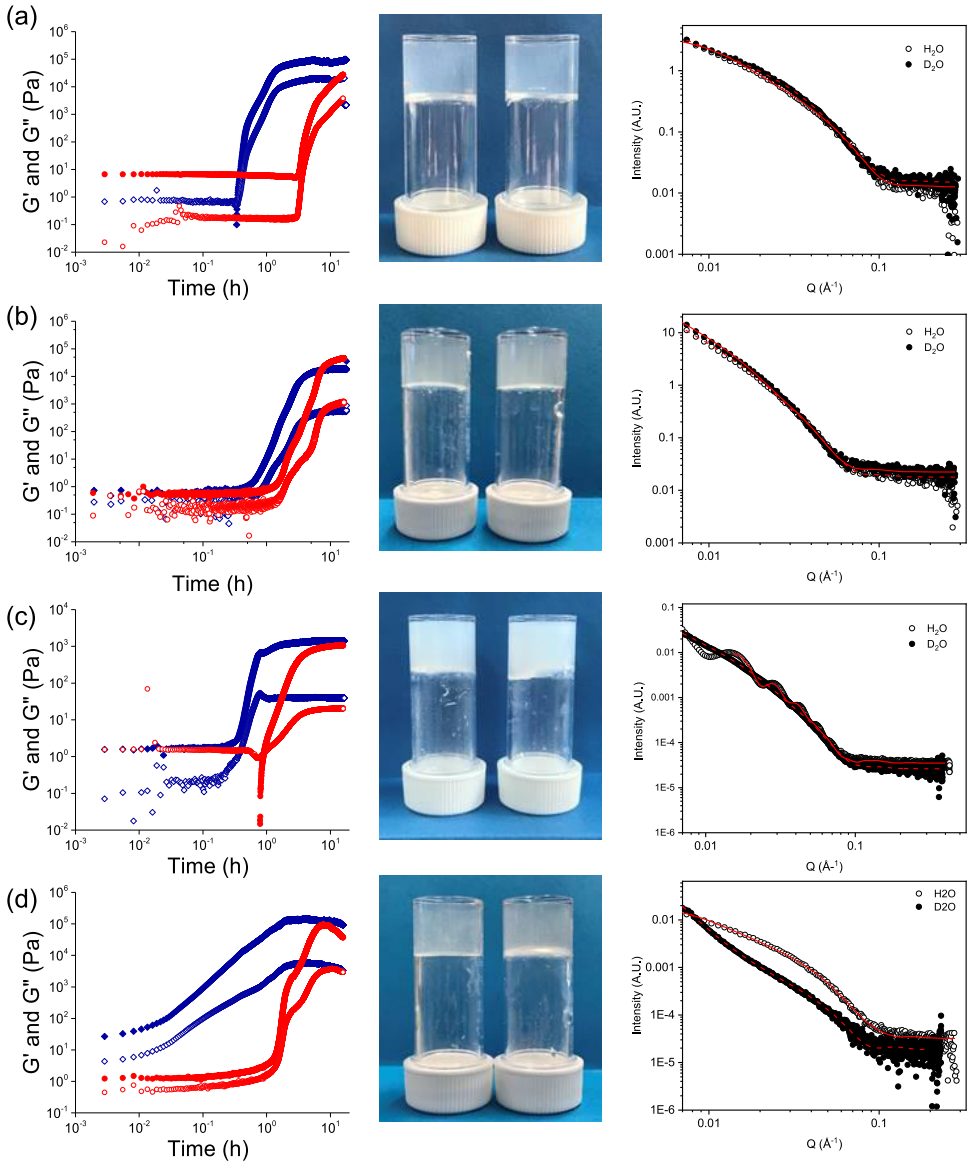

Figure 2. Time-sweep rheology data, photographs of the final gels, and SAXS data for gelation of (a) **1**, (b) **2**, (c) **3**, and (d) **4**. For rheology, the data in blue are for H_2O and the data in red are for D_2O. In all cases, closed symbols show G' and open symbols show G''. In the photographs, the left vial is for the gel in H_2O and the right vial is for the gel in D_2O. For the SAXS data, the open symbols are for the gels in H_2O and the filled symbols are for the gels in D_2O. The fits are red lines. For (d), the data have been manually rescaled as the data were collected on different instruments.

D_2O, and G' dominates over G'' from time zero. This correlates with the SAXS data showing that the structures are different at high pH. There are differences in the profile of the changes in G' and G'' with time for **4** (Figure 2d), with the sample in H_2O showing a steady change in G' and G'', whilst that in D_2O shows a two-stage process. We have previously ascribed such two-stage processes to initial fiber formation and then lateral bundling.[32]

The rheological data are determined from the mechanical properties of the primary self-assembled structures, as well as the degree of lateral association and other entanglements, which combine to give the overall gel network. The similarity in data for gels formed from **1** in H_2O and D_2O could be coincidental, with the average of very different interactions leading to an overall similar gel.[14,33] Alternatively, the similarity may suggest that the primary structures and networks are not affected by the change in solvent.

Cryo-TEM of the gel phase is problematic due to sampling issues from the stiff networks (see the discussion in the Supporting Information and Figure S5). Hence, to probe the underlying structures, we again turned to SAXS (Figure 2). For gels of **1**, the SAXS data are very similar. The data can be fitted to a flexible elliptical cylinder. This is as expected from previous work; primary fibers laterally aggregate to lead to structures where the scattering can be best fit to an elliptical shape.[31] From the fitting, the radii were 2.5 and 2.7 nm in H_2O and D_2O, with axis ratios of 2.1 and 2.2, respectively. There are differences in the Kuhn length, a measure of the structures' flexibility, with values of 25 and 95 nm for H_2O and D_2O, respectively. The lengths in both cases are again outside the range that can be probed here. These data imply that the structures in the gel phase are essentially the same in both H_2O and D_2O, with perhaps some variation in flexibility. The gels are formed at different rates and so the difference in flexibility

https://dx.doi.org/10.1021/acs.langmuir.0c01552
Langmuir 2020, 36, 8626−8631

may represent different degrees of entanglement and lateral packing resulting from how quickly charge is removed from the structures.

For gels formed from **2**, the best fit to the SAXS data is again the flexible elliptical cylinder, with the radii being very similar (4.3 and 4.6 nm in H_2O and D_2O, respectively), as are the axis ratios (3.1 and 3.3, respectively), and the Kuhn lengths (around 25 nm in both cases), with the overall length again being outside the range that can be probed by SAXS. Hence, for **2**, the structures in the gel phase are very similar in H_2O and D_2O despite the small differences in rheology.

For gels formed from **3**, the differences in the rheology data are reflected in the SAXS data. The data for the gels in H_2O can be best fitted to a hollow cylinder model, with a radius of 22 nm and a thickness of 6.5 nm. A polydispersity in the radius of 0.11 needed to be included to ensure a good fit. Hence, in H_2O, the structures in the gel phase are very similar to those in the solution state. In D_2O, however, the SAXS data can be best fitted to a flexible elliptical cylinder model with a radius of 3.2 nm and an axis ratio of 3.5. Hence, the differences in rheology can be understood in terms of different underlying structures in the two solvents.

For gels formed from **4**, the scattering data are again different from one another. The data from the gels in H_2O can be best fitted to a flexible elliptical cylinder model, with a radius of 2.9 nm and an axis ratio of 1.9. The data for the gels formed in D_2O fit best to a cylinder model combined with a power law. The cylinders have a radius of 4.0 nm. Hence, again, the differences in the rheology of the gels in H_2O and D_2O can be ascribed primarily to different structures underpinning the network.

Hence, where the underpinning structures differ, there are concomitant differences in the rheological properties. In all cases, the kinetics of the hydrolysis of GdL and hence the rate of pH decrease, and gelation are different; we cannot, therefore, relate the structural differences where they are present simply to kinetics. The rate of hydrolysis is temperature dependent.[28] However, it is not possible to simply carry out experiments at different temperatures to match the kinetics of hydrolysis in H_2O and D_2O. For this class of gelator, there can be temperature effects. For example, **1** has a different self-assembled structure at room temperature and above 40 °C, for example.[34] Likewise, it is difficult to suggest that there is a link between a single property such as hydrophobicity and whether there is an effect on changing from H_2O to D_2O. Nonetheless, we show that there is potential to use isotopic changes to control the properties of gels from a single gelator. This shows that the general assumption that there is no effect in moving between H_2O and D_2O does not always hold.

■ ASSOCIATED CONTENT

Supporting Information

The Supporting Information is available free of charge at https://pubs.acs.org/doi/10.1021/acs.langmuir.0c01552.

Full experimental details including sample preparation methods; analysis methods; further SAXS discussion and analysis; rheology data; and further TEM data (PDF)

■ AUTHOR INFORMATION

Corresponding Author

Dave J. Adams − *School of Chemistry, University of Glasgow, Glasgow G12 8QQ, U.K.*; orcid.org/0000-0002-3176-1350; Email: dave.adams@glasgow.ac.uk

Authors

Kate McAulay − *School of Chemistry, University of Glasgow, Glasgow G12 8QQ, U.K.*

Han Wang − *Department of Chemical and Biomolecular Engineering, Whiting School of Engineering, Johns Hopkins University, Baltimore, Maryland 21218, United States*

Ana M. Fuentes-Caparrós − *School of Chemistry, University of Glasgow, Glasgow G12 8QQ, U.K.*

Lisa Thomson − *School of Chemistry, University of Glasgow, Glasgow G12 8QQ, U.K.*

Nikul Khunti − *Diamond Light Source Ltd., Harwell Science and Innovation Campus, Didcot OX11 0QX, U.K.*

Nathan Cowieson − *Diamond Light Source Ltd., Harwell Science and Innovation Campus, Didcot OX11 0QX, U.K.*

Honggang Cui − *Department of Chemical and Biomolecular Engineering, Whiting School of Engineering, Johns Hopkins University, Baltimore, Maryland 21218, United States*; orcid.org/0000-0002-4684-2655

Annela Seddon − *School of Physics, HH Wills Physics Laboratory and Bristol Centre for Functional Nanomaterials, HH Wills Physics Laboratory, University of Bristol, Bristol BS8 1TL, U.K.*

Complete contact information is available at: https://pubs.acs.org/10.1021/acs.langmuir.0c01552

Notes

The authors declare no competing financial interest.

■ ACKNOWLEDGMENTS

D.J.A. thanks the EPSRC for a Fellowship (EP/L021978/1), which also funded K.M. AMFC and L.T. thank the University of Glasgow for funding. We thank Dr. Emily Draper for helpful discussions. The Ganesha X-ray scattering apparatus was purchased under EPSRC Grant "Atoms to Applications" (EP/K035746/1). This work benefitted from SasView software, originally developed by the DANSE project under NSF award DMR-0520547.

■ REFERENCES

(1) Terech, P.; Weiss, R. G. Low Molecular Mass Gelators of Organic Liquids and the Properties of Their Gels. *Chem. Rev.* **1997**, *97*, 3133−3160.

(2) Weiss, R. G. The Past, Present, and Future of Molecular Gels. What Is the Status of the Field, and Where Is It Going? *J. Am. Chem. Soc.* **2014**, *136*, 7519−7530.

(3) Draper, E. R.; Adams, D. J. Low-Molecular-Weight Gels: The State of the Art. *Chem* **2017**, *3*, 390−410.

(4) Du, X.; Zhou, J.; Shi, J.; Xu, B. Supramolecular Hydrogelators and Hydrogels: From Soft Matter to Molecular Biomaterials. *Chem. Rev.* **2015**, *115*, 13165−13307.

(5) Estroff, L. A.; Hamilton, A. D. Water Gelation by Small Organic Molecules. *Chem. Rev.* **2004**, *104*, 1201−1218.

(6) Némethy, G.; Scheraga, H. A. Structure of Water and Hydrophobic Bonding in Proteins. IV. The Thermodynamic Properties of Liquid Deuterium Oxide. *J. Chem. Phys.* **1964**, *41*, 680−689.

(7) Dougan, L.; Koti, A. S. R.; Genchev, G.; Lu, H.; Fernandez, J. M. A Single-Molecule Perspective on the Role of Solvent Hydrogen

Bonds in Protein Folding and Chemical Reactions. *ChemPhysChem* **2008**, *9*, 2836−2847.
(8) Haward, S. J.; Shewry, P. R.; Marsh, J.; Miles, M. J.; Mc Master, T. J. Force spectroscopy of an elastic peptide: Effect of D2O and temperature on persistence length. *Microsc. Res. Tech.* **2011**, *74*, 170−176.
(9) Hamley, I. W.; Burholt, S.; Hutchinson, J.; Castelletto, V.; da Silva, E. R.; Alves, W.; Gutfreund, P.; Porcar, L.; Dattani, R.; Hermida-Merino, D.; Newby, G.; Reza, M.; Ruokolainen, J.; Stasiak, J. Shear Alignment of Bola-Amphiphilic Arginine-Coated Peptide Nanotubes. *Biomacromolecules* **2017**, *18*, 141−149.
(10) Oakenfull, D.; Scott, A. Gelatin gels in deuterium oxide. *Food Hydrocolloids* **2003**, *17*, 207−210.
(11) Grant, C. A.; Twigg, P. C.; Savage, M. D.; Woon, W. H.; Greig, D. Mechanical Investigations on Agar Gels Using Atomic Force Microscopy: Effect of Deuteration. *Macromol. Mater. Eng.* **2012**, *297*, 214−218.
(12) Cardoso, M. V. C.; Sabadini, E. The gelling of κ-carrageenan in light and heavy water. *Carbohydr. Res.* **2010**, *345*, 2368−2373.
(13) Larsson, U. Polymerization and gelation of fibronogen in D2O. *Eur. J. Biochem.* **1988**, *174*, 139−144.
(14) Brenner, T.; Tuvikene, R.; Cao, Y.; Fang, Y.; Rikukawa, M.; Price, W. S.; Matsukawa, S. Hydrogen isotope replacement changes hydration and large scale structure, but not small scale structure, of agarose hydrogel networks. *Eur. Phys. J. E* **2019**, *42*, No. 53.
(15) Takahashi, H.; Ito, K. Small angle X-ray scattering study on effect of replacement of hydrogen oxide (H2O) by deuterium oxide (D2O) on anionic phospholipid bilayers. *J. Phys.: Conf. Ser.* **2007**, *83*, No. 012022.
(16) Canrinus, T. R.; Cerpentier, F. J. R.; Feringa, B. L.; Browne, W. R. Remarkable solvent isotope dependence on gelation strength in low molecular weight hydro-gelators. *Chem. Commun.* **2017**, *53*, 1719−1722.
(17) Barth, A. Infrared spectroscopy of proteins. *Biochim. Biophys. Acta, Bioenerg.* **2007**, *1767*, 1073−1101.
(18) Haris, P. I.; Chapman, D. The conformational analysis of peptides using fourier transform IR spectroscopy. *Biopolymers* **1995**, *37*, 251−263.
(19) Guilbaud, J.-B.; Saiani, A. Using small angle scattering (SAS) to structurally characterise peptide and protein self-assembled materials. *Chem. Soc. Rev.* **2011**, *40*, 1200−1210.
(20) Hollamby, M. J. Practical applications of small-angle neutron scattering. *Phys. Chem. Chem. Phys.* **2013**, *15*, 10566−10579.
(21) Makam, P.; Gazit, E. Minimalistic peptide supramolecular co-assembly: expanding the conformational space for nanotechnology. *Chem. Soc. Rev.* **2018**, *47*, 3406−3420.
(22) Draper, E. R.; Adams, D. J. Controlling the Assembly and Properties of Low-Molecular-Weight Hydrogelators. *Langmuir* **2019**, *35*, 6506−6521.
(23) Vegners, R.; Shestakova, I.; Kalvinsh, I.; Ezzell, R. M.; Janmey, P. A. Use of a gel-forming dipeptide derivative as a carrier for antigen presentation. *J. Pept. Sci.* **1995**, *1*, 371−378.
(24) Mahler, A.; Reches, M.; Rechter, M.; Cohen, S.; Gazit, E. Rigid, Self-Assembled Hydrogel Composed of a Modified Aromatic Dipeptide. *Adv. Mater.* **2006**, *18*, 1365−1370.
(25) Yang, Z.; Liang, G.; Ma, M.; Gao, Y.; Xu, B. Conjugates of naphthalene and dipeptides produce molecular hydrogelators with high efficiency of hydrogelation and superhelical nanofibers. *J. Mater. Chem.* **2007**, *17*, 850−854.
(26) Jayawarna, V.; Ali, M.; Jowitt, T. A.; Miller, A. F.; Saiani, A.; Gough, J. E.; Ulijn, R. V. Nanostructured Hydrogels for Three-Dimensional Cell Culture Through Self-Assembly of Fluorenylmethoxycarbonyl−Dipeptides. *Adv. Mater.* **2006**, *18*, 611−614.
(27) Adams, D. J.; Butler, M. F.; Frith, W. J.; Kirkland, M.; Mullen, L.; Sanderson, P. A new method for maintaining homogeneity during liquid−hydrogel transitions using low molecular weight hydrogelators. *Soft Matter* **2009**, *5*, 1856−1862.
(28) Pocker, Y.; Green, E. Hydrolysis of D-glucono-.delta.-lactone. I. General acid-base catalysis, solvent deuterium isotope effects, and transition state characterization. *J. Am. Chem. Soc.* **1973**, *95*, 113−119.
(29) Mears, L. L. E.; Draper, E. R.; Castilla, A. M.; Su, H.; Zhuola; Dietrich, B.; Nolan, M. C.; Smith, G. N.; Doutch, J.; Rogers, S.; Akhtar, R.; Cui, H.; Adams, D. J. Drying Affects the Fiber Network in Low Molecular Weight Hydrogels. *Biomacromolecules* **2017**, *18*, 3531−3540.
(30) Draper, E. R.; Wallace, M.; Schweins, R.; Poole, R. J.; Adams, D. J. Nonlinear Effects in Multicomponent Supramolecular Hydrogels. *Langmuir* **2017**, *33*, 2387−2395.
(31) Draper, E. R.; Dietrich, B.; McAulay, K.; Brasnett, C.; Abdizadeh, H.; Patmanidis, I.; Marrink, S. J.; Su, H.; Cui, H.; Schweins, R.; Seddon, A.; Adams, D. J. Using Small-Angle Scattering and Contrast Matching to Understand Molecular Packing in Low Molecular Weight Gels. *Matter* **2020**, *2*, 764−778.
(32) Cardoso, A. Z.; Alvarez Alvarez, A. E.; Cattoz, B. N.; Griffiths, P. C.; King, S. M.; Frith, W. J.; Adams, D. J. The influence of the kinetics of self-assembly on the properties of dipeptide hydrogels. *Faraday Discuss.* **2013**, *166*, 101−116.
(33) Nishinari, K.; Watase, M. Effects of sugars and polyols on the gel-sol transition of kappa-carrageenan gels. *Thermochim. Acta* **1992**, *206*, 149−162.
(34) Draper, E. R.; Su, H.; Brasnett, C.; Poole, R. J.; Rogers, S.; Cui, H.; Seddon, A.; Adams, D. J. Opening a Can of Worm(-like Micelle)s: The Effect of Temperature of Solutions of Functionalized Dipeptides. *Angew. Chem., Int. Ed.* **2017**, *56*, 10467−10470.

https://dx.doi.org/10.1021/acs.langmuir.0c01552
Langmuir 2020, 36, 8626−8631